Supporting Information

Hydration of α-UO$_3$ following storage under controlled conditions of temperature and relative humidity

Marianne P. Wilkerson,*[a] Sarah C. Hernandez,[a] W. Tyler Mullen,[a] Andrew T. Nelson,[a] Alison L. Pugmire,[a] Brian L. Scott,[a] Elizabeth S. Sooby,[a] Alison L. Tamasi,[a,b] Gregory L. Wagner,[a] and Justin R. Walensky[b]

[a]Los Alamos National Laboratory, Los Alamos, New Mexico 87545, United States
[b]Department of Chemistry, University of Missouri-Columbia, Columbia, Missouri 65211, United States

Table S1: Lattice parameters of the α-, β-, γ-, δ-, ε-, and η-UO_3, and unassigned phases of UO_3, as reported in references 16-34.

phase	reported U:O stoichio-metry	a (Å)	b (Å)	c (Å)	α (°)	β (°)	γ (°)	space group	symmetry	measure-ment	Ref.
	UO_3	3.97	3.97	4.17		120.0		$P\bar{3}m1$		XRD	16[*]
	UO_3	3.91	6.94	4.17		90.0		$C2mm$		neutron	16[*]
	UO_3	3.91	6.94	4.17		90.0		$C2$		neutron	16[*]
	UO_3	6.84	43.45	4.157				C_{222}	ortho-rhombic	neutron, electron	17[*]
	UO_{3-x}								pseudo-ortho-rhombic	XRD	18
	UO_3	3.971		4.17					hexagonal	XRD	19[*]
	UO_3	3.961 ±0.001	6.860 ±0.002	4.166 ±0.001					hexagonal	neutron	20
α-UO_3	UO_3	3.913 ±0.002	6.936 ±0.003	4.167 ±0.002					ortho-rhombic	neutron	20
	UO_3	6.878	3.971	4.168					hexagonal	XRD	21[*]
	$UO_{2.94}$	6.863	3.962	4.167					hexagonal	XRD	21[*]
	$UO_{2.71}$	6.823	3.939	4.144					hexagonal	XRD	21[*]
	$UO_{2.90}$	6.944	3.912	4.160					ortho-rhombic	XRD	21[*]
	UO_3	3.971		4.17					hexagonal	XRD	22[*]
	$UO_{2.9}$	6.91	3.92	4.16					ortho-rhombic	XRD	22[*]
	UO_3	12.98	10.70	7.49					ortho-rhombic	XRD	23[*]

Phase	Compound	a	b	c	α	β	γ	Space group	Crystal system	Method	Ref
	UO_3	3.963 ±0.004		4.160 ±0.008				$C\bar{3}m$ - D_{3d}^3	hexagonal	XRD	24
β-UO_3	UO_3	10.34	14.33	3.91		99.0		$P2_1$		XRD	16*
	UO_3	10.34	14.33	3.91		99.03			monoclinic	XRD	19*
	UO_3	10.34 ±0.01	14.33 ±0.01	3.910 ±0.004		99.03 ±0.02		$P2_1$ or $P2_1/m$	monoclinic	XRD	25
	UO_3	10.34 ±0.01	14.33 ±0.01	3.910 ±0.004		99.03 ±0.01		$P2_1$ (C_2^2) or $P2_1/m$ (C_{2h}^2)	monoclinic	XRD	26
	UO_3			14.3					ortho-rhombic?	XRD	22*
γ-UO_3	UO_3	6.90	6.90	19.98		90.0		$I4_1$		neutron	16*
	UO_3	9.79	19.93	9.71		90.0		$Fddd$		neutron	16*
	UO_3^a	6.9013(5)	6.9013(5)	19.9754(18)				$I4_1/amd$	tetragonal	neutron	27
	UO_3^b	9.787(3)	19.932(4)	9.705(3)				$Fddd$	ortho-rhombic	neutron	27
	UO_3^c	9.8225(7)	19.8487(15)	9.6318(7)				Pseudo-F_{ddd}	ortho-rhombic	neutron	27
	UO_3	9.813(8)	19.93(8)	9.711(8)				$Fddd$ - D_{2h}^{24}		XRD	28
	UO_3	9.71	9.77	19.92					ortho-rhombic	XRD	19*
	UO_3	6.89	6.89	19.94	90	90	90.34	$I4_1/amd$	tetragonal	XRD	29*
	UO_3	13.01	15.48	7.50					ortho-rhombic		22*
	UO_3	13.08	15.48	6.91		89.63			monoclinic	XRD	22*
δ-UO_3	UO_3	4.17	4.17	4.17		90.0		$Pm\bar{3}m$	cubic	neutron	16*
	UO_3	4.146(12)	4.146(12)	4.146(12)					cubic	XRD	30
	UO_3	4.165(8)	4.165(8)	4.165(8)					cubic	neutron	30
	UO_3	4.16							cubic	XRD	19*

Phase	Formula	a	b	c	α	β	γ	Space group	Crystal	Method	Ref
	UO$_3$	4.16							cubic	XRD	22*
	UO$_3$	4.138 ±0.005							cubic	XRD	31
ε-UO$_3$	UO$_3$	4.002	3.841	4.165	98.10	90.20	120.17		triclinic	XRD	19*
	UO$_3$									XRD	22
η-UO$_3$	UO$_3$	7.51	5.47	5.22		90.0		$P2_12_12_1$		XRD	16*
	UO$_3$	7.511 ±0.009	5.466 ±0.008	5.224 ±0.008				$P2_12_12_1$	ortho rhombic	XRD	32
UO$_3$	UO$_3$	4.002	3.841	4.165	98°17′	90°33′	120°28′		triclinic	XRD	33*
	UO$_3$	13.05 ±0.02	15.45 ±0.05	6.89 ±0.02		89.63 ±0.01			monoclinic	XRD	34

*No error reported.
[a]measured at 373 K
[b]measured at 323, 293 K
[c]measured at 77 K

Note: Zachariasen assigned the α-UO$_3$ structure to hexagonal $P\bar{3}m1$.[16] Following XRD and neutron diffraction analyses, Loopstra and Cordfunke proposed that the hexagonal assignment was incorrect, and then prepared UO$_{2.9}$ by thermal decomposition of uranyl peroxide at 450 °C in the absence of nitrate.[20] After cooling to room temperature, the UO$_{2.9}$ formed orthorhombic α-UO$_3$ characterized by a space group of C2mm.[20] The discrepancy between the densities reported by Hoekstra and Siegel (7.04 g cm^{-3}),[22] Loopstra and Cordfunke (7.25 g cm^{-3}),[20] and Siegel and Hoekstra (7.30 g cm^{-1})[18] versus the density also calculated by Seigel and Hoekstra (8.39 g cm^{-3}) led Greaves and Fender to characterize α-UO$_3$ as an imperfect orthorhombic C222 structure in which ~12% of the U lattice sites are vacant.[17] In models reported separately by Greaves versus Loopstra and Cordfunke, axial oxygen (O1) sites contribute to the –oxo-U-oxo-U-oxo- chains, and equatorial oxygen (O2) sites lie in the equatorial (110) plan.[17,20] The O2 atoms occupy slightly distorted hexagonal bipyramidal coordination along the (001) plane. Due to the complexity of the C222 model, we chose to use the orthorhombic C2mm structure proposed by Loopstra and Cordfunke for our simulations.[20]

Table S2: Lattice parameters of hydrated UO_3 species, as reported in references 21, 35-50.

reported UO_2:H_2O stoi-chiometry	species	a (Å)	b (Å)	c (Å)	β (°)	space group	symmetry	measure-ment	Ref.
$UO_3 \cdot 2.25H_2O$	$[(UO_2)_8O_2(OH)_{12}](H_2O)_{12}$	14.337(3)	16.813(4)	14.731(4)		$P2_1ca$	ortho-rhombic	XRD	35
$UO_3 \cdot 2H_2O$	$(UO_2)_4O(OH)_6 \cdot 5H_2O$	14.6861(4)	13.9799(3)	16.7063(5)		$Pbcn$	ortho-rhombic	XRD	36
	α-$UO_3 \cdot 2H_2O$							XRD	21
	β-$UO_3 \cdot 2H_2O$						ortho-rhombic	XRD	21
		13.977 ±0.004	16.696 ±0.004	14.672 ±0.004			ortho-rhombic		37
	$UO_3 \cdot 2H_2O$	13.997(4)	16.696(4)	14.672(4)		$Pbna$	ortho-rhombic		38
								EXAFS	39
$UO_3 \cdot H_2O$	α-$UO_2(OH)_2$	4.2455(6)	10.3183(16)	6.8648(10)		$Cmca$ or $C2cb$			40
		4.242(1)	10.302(1)	6.868(1)		$Cmca$ or $C2cb$	ortho-rhombic	XRD	38, 41, 42
								neutron	42
							ortho-rhombic	XRD	43
	β-$UO_2(OH)_2$	5.6438(1)	6.2867(1)	9.9372(2)		$Pbca$	ortho-rhombic	XRD	38, 40
		5.6438 ±0.0001	6.2867 ±0.0001	9.9372 ±0.0002		$Pbca$	ortho-rhombic	XRD	44

		a	b	c	angle	space group	crystal system	method	ref
								neutron	42, 45
		6.295 ±0.005	5.636 ±0.005	9.92 ±0.01		*Fmmm*	ortho-rhombic	XRD	46
	γ-$UO_2(OH)_2$	6.419(2)	5.518(2)	5.561(2)	112.77	$P2_1/c$	monoclinic	XRD	38
		5.560(3)	5.522(3)	6.416(3)	112.71	P2$_1$/c	monoclinic	XRD	47
								XRD	21
							hexagonal	XRD	43
	δ-$UO_2(OH)_2$							XRD	21
							triclinig	XRD	43
	ε-$UO_3 \cdot H_2O$	6.419 ±0.002	5.518 ±0.002	5.561 ±0.002	112°46' ±3'	$C_m(C_s^3)$, $C2(C_2^3)$ or $C2/m$ (C_{2h}^3)	monoclinic	XRD	48
	$UO_2(OH)_2$	5.635 ±0.007	6.285 ±0.008	9.919 ±0.008		*Pbca*	ortho-rhombic	XRD	49
		5.638 ±0.005	6.273 ±0.005	9.925 ±0.005		*Pbca*	ortho-rhombic	XRD	50
$UO_3 \cdot 0.08H_2O$	α-$UO_3 \cdot 0.8H_2O$	4.27-4.30(1)	10.19-10.24(1)	6.86-6.96(1)			ortho-rhombic	XRD	38
	β-$UO_3 \cdot 0.8H_2O$						ortho-rhombic	XRD	21
	$UO_3 \cdot 0.8H_2O$	10.23 ±0.01	6.89 ±0.01	4.28 ±0.01			ortho-rhombic	XRD	50

Table S3: Conditions (temperature, relative humidity), resultant water vapor density, and salt used to prepare saturated aqueous solutions used for storage of α-UO$_3$ subsamples.[11,59-61]

condition	temperature (°C)	relative humidity (%)	water vapor density (g/cm³)	salt used to prepare saturated aqueous soltuion
1	5	25	1.7 x 10^{-6}	lithium iodide
2	37	15	6.6 x 10^{-6}	lithium iodide
3	5	97	6.7 x 10^{-6}	potassium nitrate
4	37	89	39 x 10^{-6}	potassium nitrate

Table S4: Fit results of α-UO$_3$ at time 0 and after 0.5 years of storage under Condition 1, Condition 2, Condition 3, and Condition 4. The k^3-weighted U L$_{III}$-edge data are transformed between k = [2.5 – 15.0 Å^{-1}] and narrowed by a Gaussian window of 0.3 Å^{-1}. Fit range is between R = [1.5 Å – 6.5 Å]; S_0^2 is constrained to 1.0; and the number of scatterers N, the distance R, and the Debye-Waller factor are varied. A multiple scattering path summing all the high R multiple scattering paths (R > 4.5 Å) was included. Reported errors are determined using a Monte Carlo method and primarily reflect reproducibility.[76] Absolute errors for σ^2 and R are ~ 10% and 0.005 Å for near neighbors, and 20% and 0.02 Å for further neighbors, respectively.

	time 0			time 0.5 years Condition 1			time 0.5 years Condition 2		
U L$_{III}$ edge	N	R(Å)	σ^2(Å^2)	N	R(Å)	σ^2(Å^2)	N	R(Å)	σ^2(Å^2)
U-O	-	-	-	1.1	1.667	0.0030	1.3	1.765	0.0025
U-O	0.5	1.926	0.0100	1.1	2.111	0.0029	3.3	2.034	0.0040
U-O	2.6	2.220	0.0025	2.2	2.269	0.0022	-	-	-
U-O	0.1	2.482	0.0025	1.7	2.540	0.0050	4.2	2.649	0.0049
U-U	7.2	3.779	0.0096	-	-	-	-	-	-
U-U	6.9	4.162	0.0031	0.6	4.124	0.0025	1.9	4.035	0.0069
ΔE$_o$ R(%)		-13.0 31			-4.4 24			10 27	
				time 0.5 years Condition 3			time 0.5 years Condition 4		
U L$_{III}$ edge				N	R(Å)	σ^2(Å^2)	N	R(Å)	σ^2(Å^2)
U-O				2.0	1.763	0.2500	2.3	1.760	0.0027
U-O				5.0	2.033	0.0045	3.6	2.038	0.0026
U-O				2.9	2.347	0.0040	3.7	2.360	0.0047
U-O				2.9	2.662	0.0029	1.9	2.689	0.0025
U-U				-	-	-	-	-	-
U-U				2.9	4.036	0.0099	2.3	4.072	0.0081
ΔE$_o$ R(%)					6.9 20			2.1 20	

Table S5: Fit results of α-UO$_3$ at time 0 and after 3 years of storage under Condition 1, Condition 2, Condition 3, and Condition 4. The k^3-weighted U L$_{III}$-edge data are transformed between k – [2.5 – 15.0 Å^{-1}] and narrowed by a Gaussian window of 0.3 Å^{-1}. Fit range is between R = [1.5 Å – 6.5 Å] with N, R, and σ^2 varying and S_0^2 fixed to 1.0. Reported errors are similar to those reported in Table S-4.

	time 0			time 3 years Condition 1			time 3 years Condition 2		
U L$_{III}$ edge	N	R(Å)	σ^2(Å²)	N	R(Å)	σ^2(Å²)	N	R(Å)	σ^2(Å²)
U-O	-	-	-	1.1	1.842	0.0025	1.3	1.767	0.0050
U-O	0.5	1.926	0.0100	0.9	2.145	0.0025	3.3	2.040	0.0025
U-O	2.6	2.220	0.0025	-	-	-	-	-	-
U-O	0.1	2.482	0.0025	1.6	2.715	0.0062	4.0	2.643	0.0034
U-U	7.2	3.779	0.0096	1.0	3.831	0.0025	-	-	-
U-U	6.9	4.162	0.0031	3.6	4.186	0.0025	0.9	3.979	0.0025
ΔE$_o$ R(%)		-13.0 31			-10 23			10 26	

				time 3 years Condition 3			time 3 years Condition 4		
U L$_{III}$ edge				N	R(Å)	σ^2(Å²)	N	R(Å)	σ^2(Å²)
U-O				1.8	1.764	0.0025	1.9	1.770	0.0025
U-O				3.6	2.063	0.0025	4.8	2.032	0.0047
U-O				3.5	2.362	0.0025	2.2	2.345	0.0025
U-O				1.4	2.715	0.0100	4.6	2.668	0.0100
U-U				-	-	-	-	-	-
U-U				1.5	4.031	0.0025	2.3	4.009	0.0085
ΔE$_o$ R(%)					1.6 38			1.6 25	

Table S6. Lattice constants a, b, c, α, β, and γ of the lattice constants from those of the theoretically relaxed α-UO$_3$ structure following addition of 1, 2 or 3 interstitial H$_2$O molecules or 1, 2 or 3 interstitial OH groups into the relaxed α-UO$_3$ lattice.

	a (Å)	b (Å)	c (Å)	$\%\Delta a$	$\%\Delta b$	$\%\Delta c$	α (°)	β (°)	γ (°)
Theoretical	3.953	6.827	4.177	-	-	-	90	90	90
1 H$_2$O	4.296	6.384	4.264	8.323	-6.701	2.076	93.635	90.269	87.903
2 H$_2$O	4.286	7.175	4.321	8.090	4.981	3.392	90.206	93.758	90.100
3H$_2$O	4.021	7.459	4.325	1.700	8.859	3.498	92.764	93.984	90.648
1 OH	4.368	6.495	4.307	9.980	-4.974	3.067	94.558	90.156	93.055
2 OH	4.321	6.490	4.519	8.905	-5.052	7.885	89.475	89.774	90.879
3 OH	4.231	7.628	4.251	6.803	11.088	1.776	90.153	90.729	101.149

Table S7. Average U-O1 and U-O2 bond lengths and U-U distances calculated for relaxed structures of α-UO$_3$ following addition of 1, 2 or 3 interstitial H$_2$O molecules and 1, 2 or 3 interstitial OH groups into the α-UO$_3$ lattice. Numbers in the parentheses indicate the percent of U-O1, U-O2 and U-U bonds that are the theoretical bonds in unperturbed α-UO$_3$.

	U-O1 (Å)	U-O2 (Å)	U-U (Å)
Experimental	2.083	2.096	3.961
Theoretical	2.088	2.279	3.947
1 H$_2$O	1.895 (43.06%)	1.892 (20.37%)	3.801 (32.61%)
2 H$_2$O	1.873 (41.67%)	2.036 (40.74%)	3.766 (16.85%)
3 H$_2$O	1.876 (40.28%)	1.876 (13.43%)	3.761 (17.93%)
1 OH	1.876 (40.28%)	2.023 (37.96%)	3.814 (28.80%)
2 OH	1.848 (40.28%)	1.848 (13.43%)	3.783 (26.63%)
3 OH	1.894 (40.28%)	2.001 (36.57%)	3.732 (15.22%)

Table S8: Final state, bond lengths and angles of initial 1, 2 or 3 H_2O molecules and 1, 2 or 3 OH groups after relaxation.

Initial	Final	O-H (Å)	O-H-O (°)	O2-H (Å)	O2-H-O2 (°)	O-O2 (Å)
1 H_2O	1 H_2O	0.992, 1.026	109.867	-	-	-
2 H_2O	4 OH, 1 O_2	0.982	-	0.979, 0.982, 1.002	-	1.447
3H_2O	2 H_2O, 2 OH, 2 O_2	0.975, 1.010	107.028	0.978, 0.986, 1.001, 1.020	112.469	1.387, 1.441
1 OH	1 OH	0.990	-	-	-	-
2 OH	2 OH, 1 O_2	1.009	-	0.981	-	1.474
3 OH	3 OH, 2 O_2	0.985	-	0.988, 0.998	-	1.424, 1.474
Experimental	OH^-	0.970	-	-	-	-
	H_2O	0.958	104.450	-	-	
	O_2^{2-}	-	-	-	-	1.447

Figure S1. Fourier Transforms (FTs) of U L$_{III}$ EXAFS data (solid black line) and fit (dashed black line) for α-UO$_3$ at time 0.
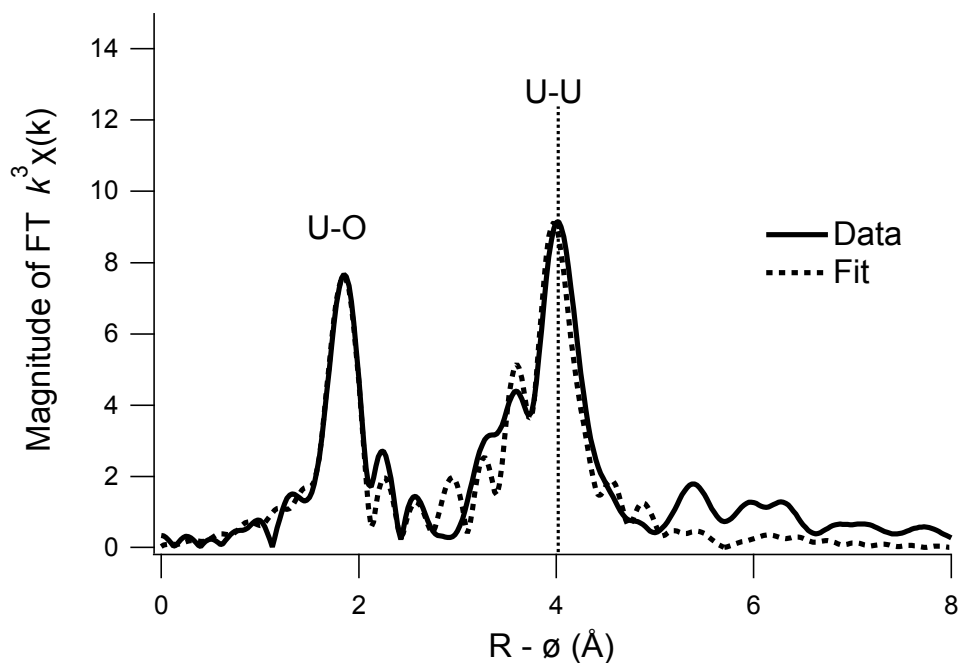
Figure S2. Fourier Transforms (FTs) of U L$_{III}$ EXAFS data for α-UO$_3$ after storage for 0.5 years under Condition 1. Data is shown as solid lines; fits to the data are displayed as dashed lines.
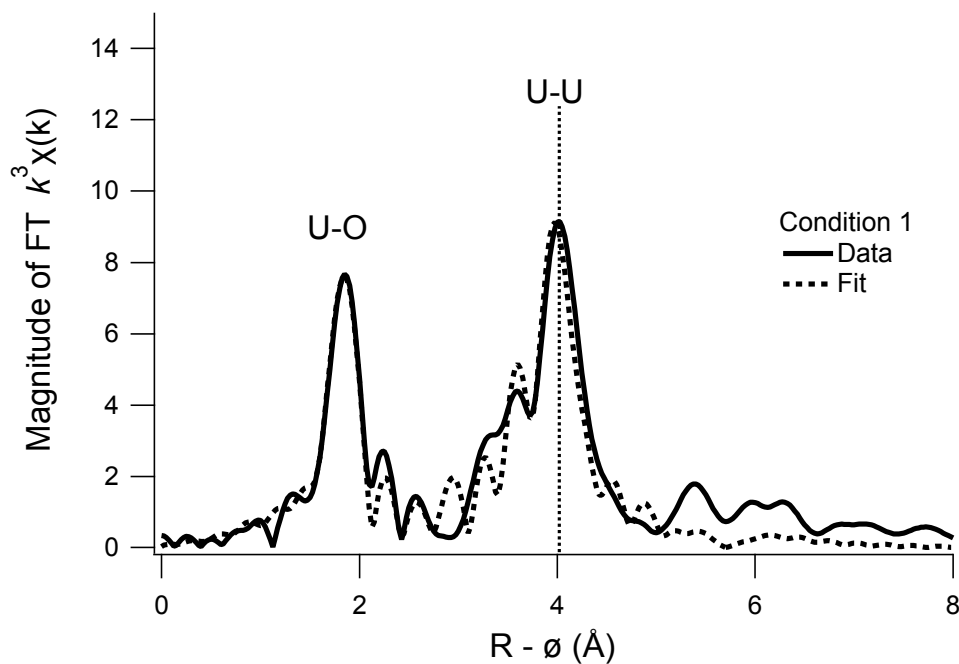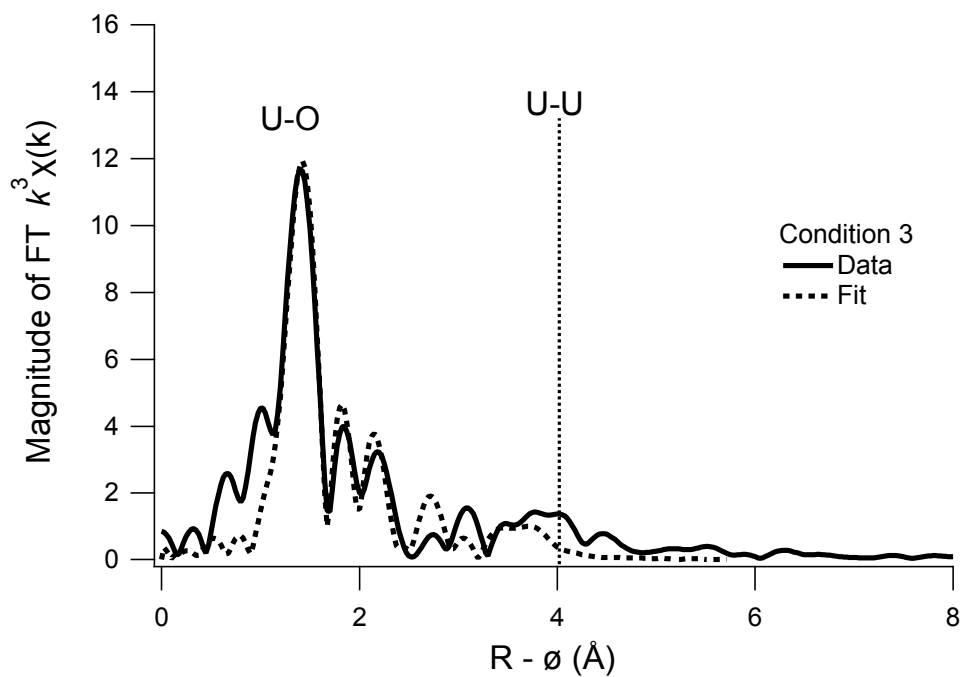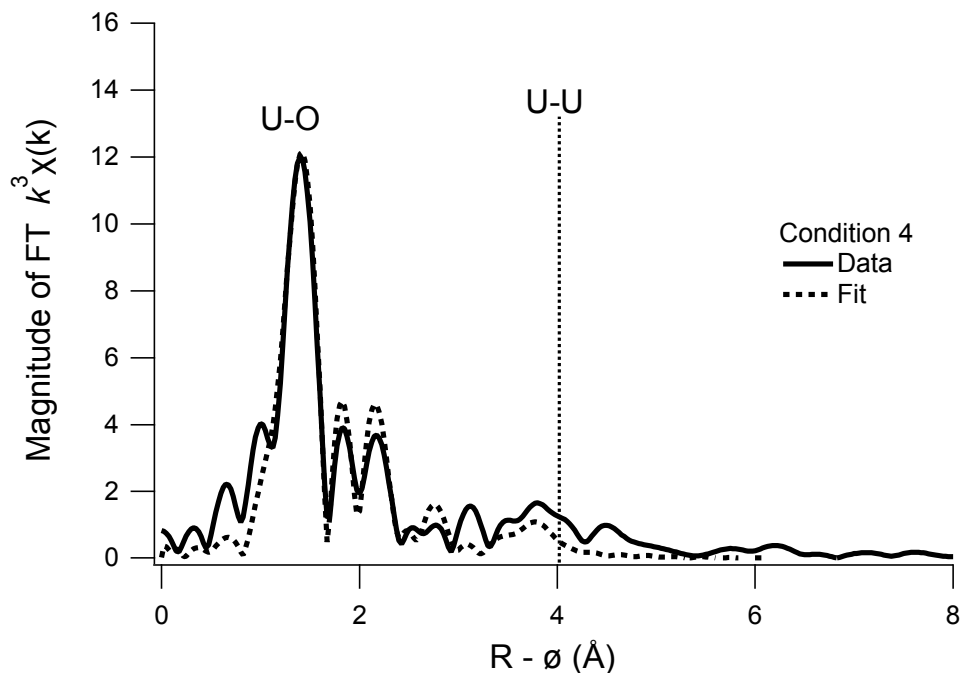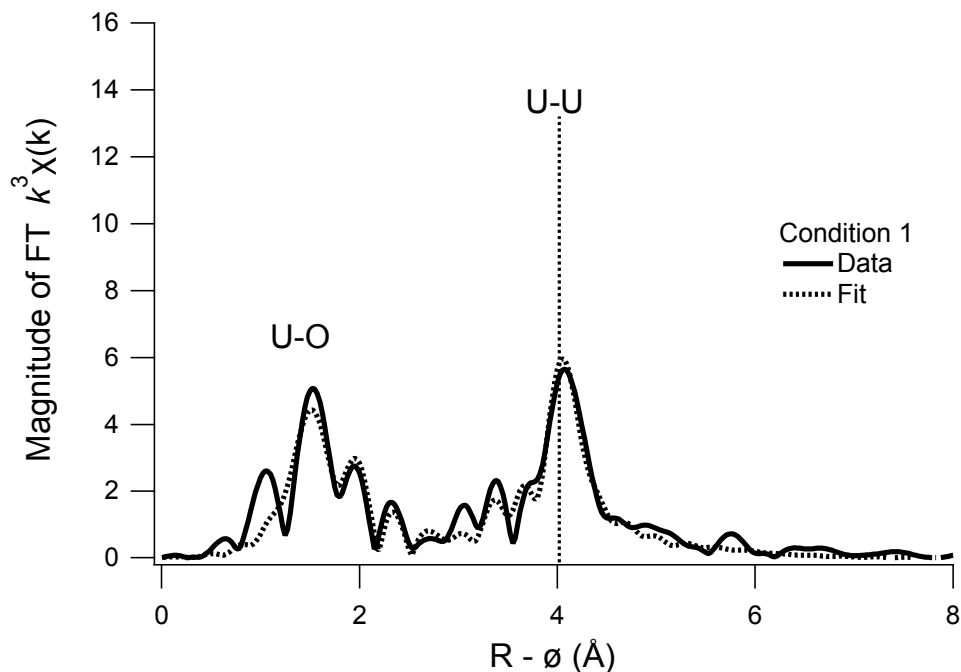
Figure S3. Fourier Transforms (FTs) of U L$_{III}$ EXAFS data for α-UO$_3$ after storage for 0.5 years under Condition 2. Data is shown as solid lines; fits to the data are displayed as dashed lines.
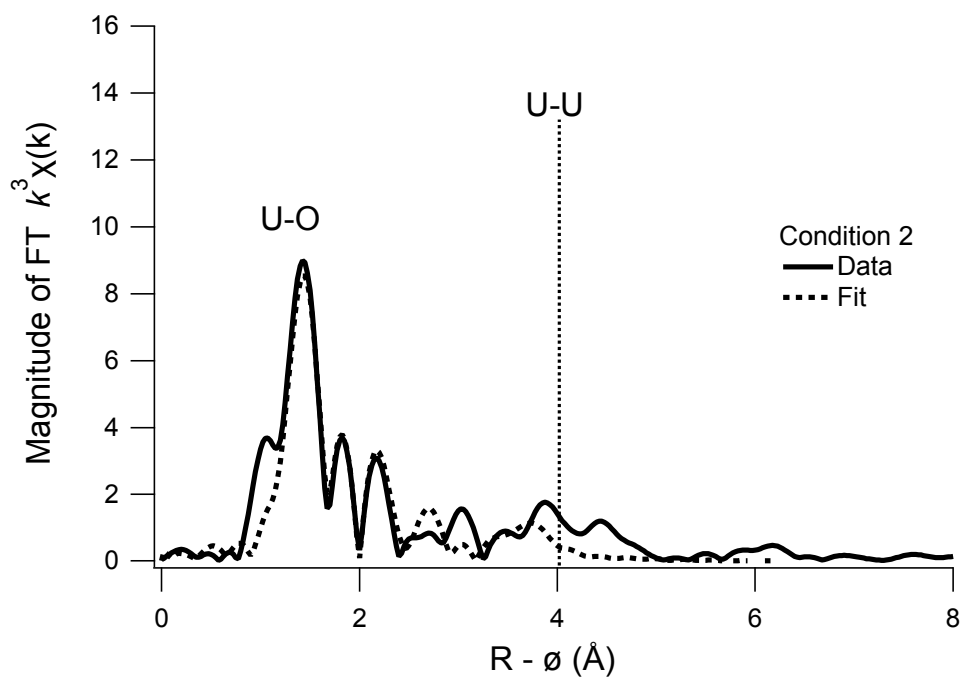
Figure S4. Fourier Transforms (FTs) of U L$_{III}$ EXAFS data for α-UO$_3$ after storage for 0.5 years under Condition 3. Data is shown as solid lines; fits to the data are displayed as dashed lines.
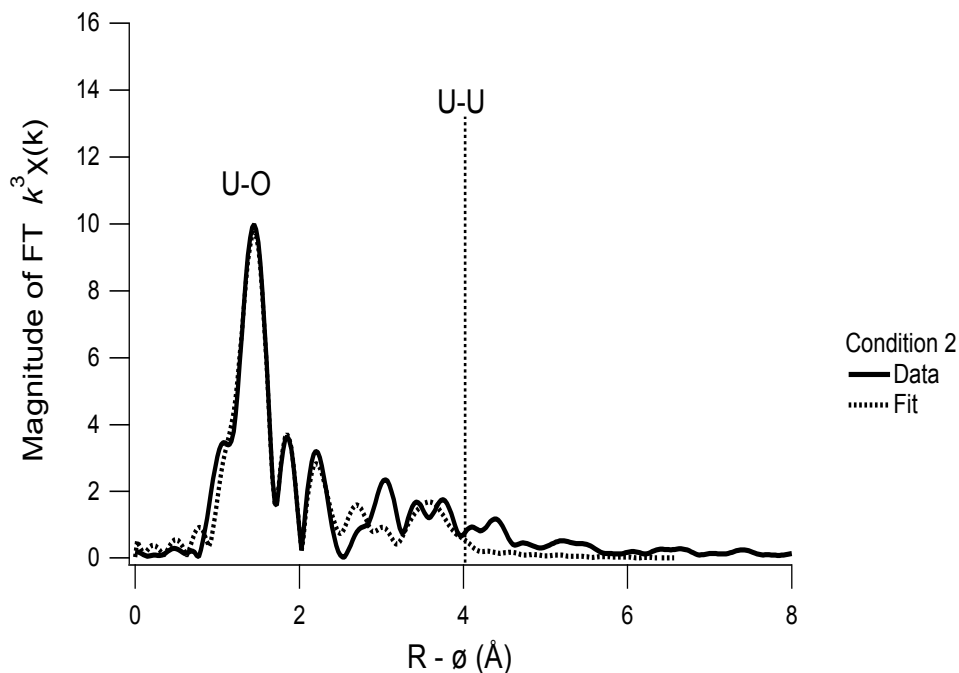
Figure S5. Fourier Transforms (FTs) of U L$_{III}$ EXAFS data for α-UO$_3$ after storage for 0.5 years under Condition 4. Data is shown as solid lines; fits to the data are displayed as dashed lines.

Figure S6. Fourier Transforms (FTs) of U L$_{III}$ EXAFS data for α-UO$_3$ after storage for 3 years under Condition 1. Data is shown as solid lines; fits to the data are displayed as dashed lines.
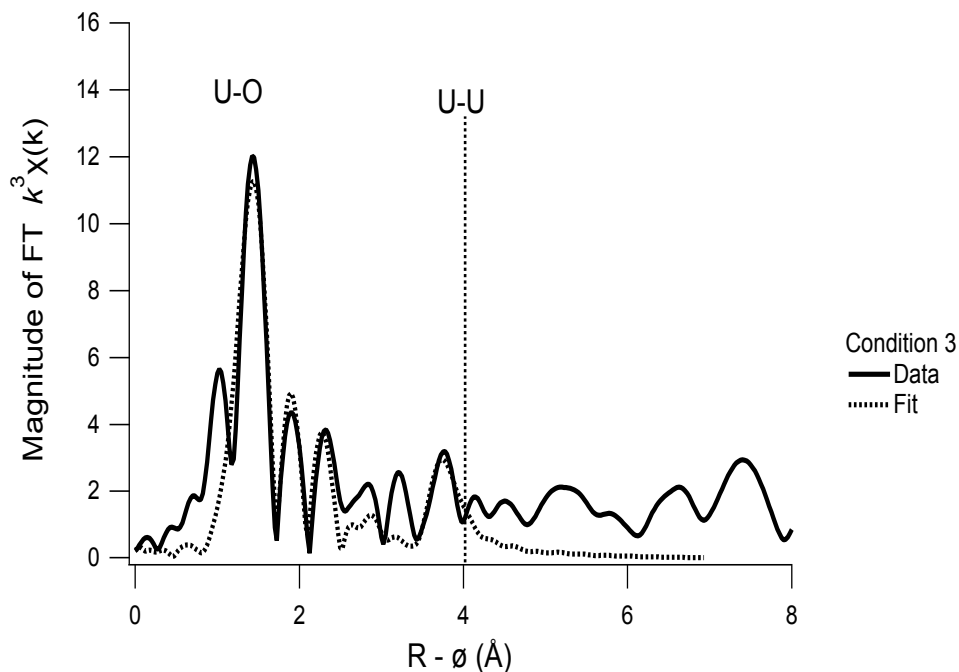
Figure S7. Fourier Transforms (FTs) of U L_{III} EXAFS data for α-UO_3 after storage for 3 years under Condition 2. Data is shown as solid lines; fits to the data are displayed as dashed lines.

Figure S8. Fourier Transforms (FTs) of U L_{III} EXAFS data for α-UO_3 after storage for 3 years under Condition 3. Data is shown as solid lines; fits to the data are displayed as dashed lines.

Figure S9. Fourier Transforms (FTs) of U L$_{III}$ EXAFS data for α-UO$_3$ after storage for 3 years under Condition 4. Data is shown as solid lines; fits to the data are displayed as dashed lines.
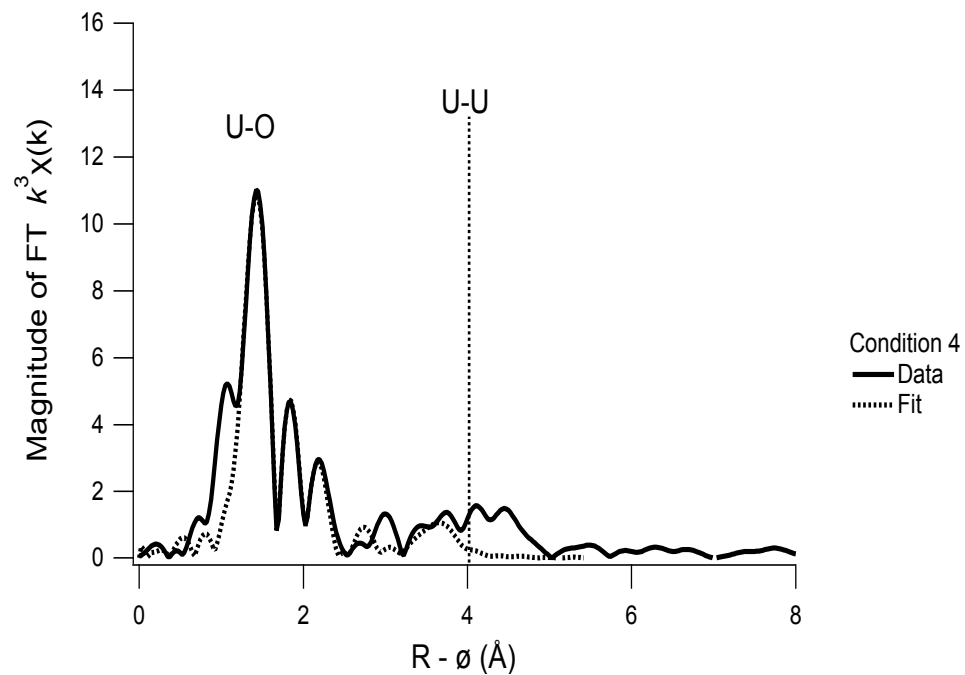
Figure S10. X-ray diffraction pattern of α-UO_3 sample stored under Condition 1 for 5 years. The composition is predominantly α-UO_3 as indicated by the orange peak markers for PDF 00-012-0043. The arrow indicates a small contribution from $UO_3 \cdot xH_2O$ type phases.